Full Paper

Israel Journal of Chemistry

DOI: 10.1002/ijch.201700142

Birth and Death of Invading Standing Waves in the BZ-AOT Reaction-diffusion System

Delora K. Gaskins,[a] Jamie S. Soohoo,[a] Milos Dolnik,[a] and Irving R. Epstein*[a]

Abstract: We report our experimental observation of modulated standing waves that invade bulk oscillations exhibited by the Belousov-Zhabotinsky-Aerosol OT reverse microemulsion system. The modulated standing waves form within domains bounded by a traveling wave. We also observe that the modulated standing waves give way to traveling waves, which we connect to numerical simulations in a simple chemical model.

Keywords: Belousov-Zhabotinsky reaction · BZ-AOT system · standing waves · reaction-diffusion

1. Introduction

There are many examples of oscillations and pattern formation in the natural world as well as in engineered systems. Patterns emerge from the temporally stationary, spatially homogeneous state *via* a variety of fundamental instabilities and bifurcations, including the Hopf bifurcation, the Turing instability,[1] and the wave instability. In the spatially independent Hopf bifurcation, as the bifurcation parameter is changed the stable steady state becomes unstable and a stable limit cycle emerges, leading to oscillation of the system in time. In the classic Turing instability, the uniform steady state is destabilized by the Fickian diffusion[2] of the components, and finite wavelength perturbations can grow, resulting in the development of patterns that are stationary in time and periodic in space, with an intrinsic wavelength. Turing also predicted the formation of waves which are oscillatory in time and periodic in space in his reaction-diffusion model.[1]

Systems are not limited to one of these instability types, but rather can exhibit pattern formation involving multiple instabilities interacting within a given domain, *e.g.*, in oscillatory Turing patterns.[3–6] When there are multiple instabilities, the system can also form pattern domains with different patterns, such as adjacent domains of Turing patterns and bulk oscillations arising *via* a Hopf bifurcation.[7] Even with only a single instability, multiple point sources can form subdomains that interact. Standing wave patterns can form when there are multiple sources of wavetrains within a given domain. Standing waves were first observed in reaction-diffusion chemical systems in the heterogeneous catalytic oxidation of carbon monoxide on a platinum surface.[8,9]

Turing patterns, bulk oscillations and waves have been observed in the Belousov-Zhabotinsky (BZ) reaction incorporated into an AOT (dioctyl sodium sulfosuccinate) reverse microemulsion. Multiple types of waves have been observed in this system, including standing waves.[10,11] Localized domains of standing waves have also been reported.[12] Standing waves whose antinodes are slightly out of synchronization with their neighbors are known as modulated standing waves and have been predicted to form as a result of interaction[13] between Hopf and wave instabilities.[14]

In this work, we present experimental results on the birth (invasion into a spatially homogeneously oscillating region) of standing waves and their death (transition to spirals) in a closed system. We show an invasion pathway for localized structures to form standing waves that overtake the Hopf domain. The standing waves occur in a region bounded by a traveling wave envelope that separates the invading standing waves from the Hopf domain. We also examine the transition of the standing waves to spiral structures and connect this to a generic chemical model.

2. Experimental

All reagents were purchased from Sigma-Aldrich, except AOT, which was obtained from ACROS Fisher. Cyclooctane was purified by combining it with sulfuric acid for at least two days, until the aqueous layer was a dark orange color. Two different microemulsion stock solutions were prepared in order to prevent the BZ components from reacting prematurely. The first microemulsion (ME I) contained malonic acid (MA), and sulfuric acid, and the second (ME II) contained sodium bromate and ferroin. ME I and ME II were prepared to have the same dispersed volume fraction ϕ_d (combined volume of the surfactant and water as a fraction of the total volume) and were stirred for more than 45 min. The time elapsed between mixing aliquots of ME I and ME II with cyclooctane to the desired ϕ_d and transferring the reacting microemulsion to the reactor was approximately 1 min. Unless otherwise noted, the concentrations of the BZ reactants in the aqueous phase of the

[a] D. K. Gaskins, J. S. Soohoo, M. Dolnik, I. R. Epstein
Department of Chemistry, Brandeis University,
Waltham, MA, USA 02453
E-mail: epstein@brandeis.edu

Supporting information for this article is available on the WWW under https://doi.org/10.1002/ijch.201700142

reacting microemulsion were [MA] = 0.25 M, [H_2SO_4] = 0.40 M, [$NaBrO_3$] = 0.20 M, and [ferroin] = 0.01 M. The [water]/[AOT] ratio of the reacting microemulsion is w. The threshold for ME I to form a thermodynamically stable reverse microemulsion is near this set of conditions. Increasing the sulfuric acid concentration slightly or decreasing the surfactant AOT leads to a turbid mixture. The aging of the batches of AOT and cyclooctane has also been observed to affect this threshold and to shift the patterns' location in the parameter space.

Experiments on a thin layer of reactive solution were carried out using two glass windows separated by a Teflon gasket of 0.09 mm thickness. The wavelength of the pattern can vary slightly over the observed domain, but is typically greater than the gasket thickness by a factor of about 2. The glass windows were contained in a sealed reactor body. It should be noted that when localized spots appeared prior to the screwing on of the reactor cap to the rest of the reactor body, the circular spots became elongated along one axis. A 5.2 cm 3 5.2 cm LED light unit (CCS Inc.) was placed underneath the reactor to allow images of the transmitted light to be captured by a charge-coupled device (CCD) camera.

The camera was fitted with a 532 nm bandpass filter. The concentration ratio of the oxidation states of the catalyst, ferroin (reduced, red) and ferriin (oxidized, blue), determines the color of the system. White in the images corresponds to the blue state, with the darkness of the image increasing with the concentration of the reduced state of the catalyst. Images were captured at one image per second. MATLAB was used to make space-time plots of the patterns. Simulations were performed in COMSOL.

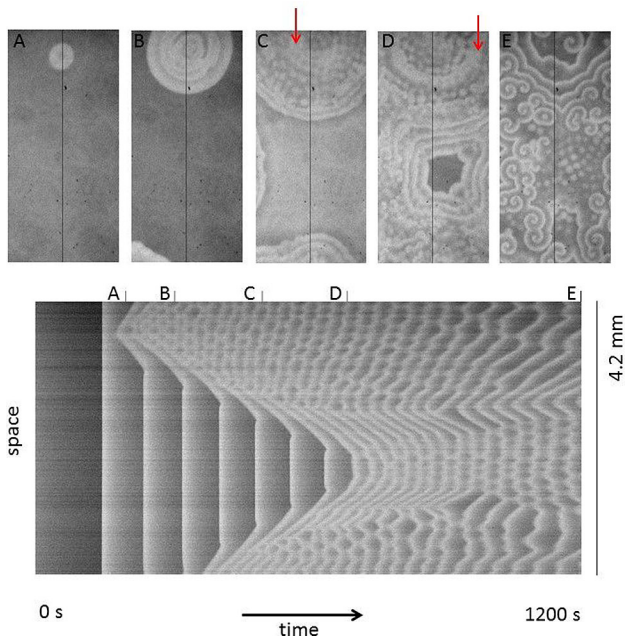

Figure 1. Invasion of modulated standing waves into into the bulk oscillation region. Images A–E show the invasion of the spatial patterns from the edges into the bulk oscillation region in the center. These images correspond to the times marked in the space-time plot below. The space line in the space-time plot is the vertical dark line in the series of images. Total time elapsed is 1200 s. Images are 2 mm 3 4.2 mm. The parameters w and f_d are 12.35 and 0.45, respectively. The greyscale reflects the ratio of ferriin to ferroin, with the light regions corresponding to high [ferriin] and dark ones to high [ferroin].

3. Results and Discussion

3.1 Birth of Standing Waves

Localized spot structures form in a bulk oscillation region and evolve to form expanding circular domains of standing wave and modulated standing wave structures in Figure 1. The oscillations are relaxational in nature. The first spike of oxidation occurs in the bulk just before formation of the expanding circular front, which is shown in (A). The elapsed time between the oxidation spikes in the bulk shortens as time progresses. The front separating the spatial structures from the homogeneous region speeds up as the bulk relaxes. Standing wave formation occurs behind the expanding front (B). A lattice structure then forms, as seen in (C).

The expanding circular front also leaves behind an excited region that propagates inward. This can be seen in the space-time plot just after the indicating mark for image (A) and in the supplemental video. This is reminiscent of the backfiring behavior observed in numerics and experiments on chemical systems.[15–18]

Modulated standing waves (MSW) are observed to evolve from the standing waves as a difference of phase develops within the domain. The antinodes of the lattice of standing waves are oscillating and annihilate with the waves of the neighboring antinodes. The modulation separates the domain into zones of (i) white spots with dark background or (ii) white background with some dark spots. The centers of the spots are the antinodes of the standing waves. The desynchronization appears to travel in the direction opposite to the expanding traveling wave. A series of zones of type (ii) appear to be moving inward, as seen in the supplemental video for this figure.

The oxidized zone, which is marked with arrows, is forming in (C) and becomes clearer in (D). This is seen in the space-time plot of the standing waves, which are initially oriented vertically (*i. e.*, in-phase). Then, near the mark for (B), they lose synchrony with their neighbors, creating the zones described above, which results in an apparent direction of propagation indicated by the development of a slope in the modulated waves. Also shown in image (D) is the formation of traveling waves near the center of the image between the standing wave structures. Spiral structures form in the domains of the standing wave structures. The space-time plot shows that the traveling waves that form at the boundary of a standing wave domain interfere to produce standing wave structures. These standing waves and spirals are shown in (E).

A notable, and typical feature of the invasion of the standing wave structures can be observed in Figure 2. The spatially localized spots that ultimately form standing waves appear at the same time, just prior to the peak of the relaxation oscillation. The upper four space-time plots in Figure 2 illustrate this behavior. Not all of the expanding structures form standing waves from the beginning; for example, a target pattern is shown in the lowermost space-time plot (E).

The invasions presented in Figures 1 and 2 do not involve the oxidized uniform state. Instead, there are circular waves of oxidation that propagate into the bulk. The standing waves develop behind that front. The leading front is observed to speed up rather than propagating at a constant speed. This is due to the interaction of the leading front and the oscillations in the bulk medium. We also note that the interference of the traveling waves in Figure 1 is not typical for trigger waves, in which the leading fronts annihilate, as they cannot propagate into each other's refractory region.

This invasion type differs from the localized standing waves that invade the bulk oscillations of the BZ-AOT[19] and CO oxidation[9] systems, which do not have a defined wave envelope as a front between the bulk oscillation and standing waves. Figure 2 shows that multiple localized wave domains occur at the same time. We interpret this behavior as resulting from the spatially distributed noise that is always present in the experimental system acting as a perturbation that can grow within certain excitable windows in the phase of the bulk oscillation.

3.2. Death of Modulated Standing Waves

In our experiments, the BZ-AOT experimental medium is a far-from-equilibrium dynamical system within a batch reactor, and so over time the system must approach and ultimately reach equilibrium. Previous experiments in the BZ-AOT system have shown that standing waves can transition to traveling waves.[10,11] The wavelength of the pattern was halved in the transition observed by Kaminaga *et al.*, and transitions to spirals and packet waves were reported by Bánsági *et al.* While there have been numerical investigations of standing waves[10,11,19] and modulated standing wave behavior[13,20] in chemical reaction-diffusion systems, the transitions studied have not, to our knowledge, included spiral formation. Peña and Bestehorn[13] used the following three-variable model to observe the interaction between Hopf and wave instabilities, generating modulated standing waves and different types of spirals, depending on the proximity to the codimension-2 point of the instabilities. The variables U, V, and W represent chemical species with diffusion coefficients D_U, D_V, *and* D_W, respectively. A and B are input reactants of the model, and p is a ratio of kinetic rate constants.

$$\frac{\partial U}{\partial t} = -2U + 3BW + D_U\nabla^2 U \tag{1}$$

$$\frac{\partial V}{\partial t} = U - VW^2 + D_V\nabla^2 V \tag{2}$$

$$\frac{\partial W}{\partial t} = A - (3B + p)W + 2VW^2 + D_W\nabla^2 W \tag{3}$$

We have used their model to qualitatively reproduce the transition we observe experimentally in our chemical system of modulated standing waves to spiral structures. We achieve this by perturbing the system far enough from the U variable steady state with random spatial noise. The noise is added only in the initial condition, and the parameters do not change over time. The space-time plot in Figure 3A shows initial bulk oscillations and the formation of modulated standing waves. As time progresses, a single spiral forms, which then proceeds to overtake the rest of the domain. An experiment is shown on the right for comparison. In the experiment, the spiral formation arises well before the desynchronization of the standing waves and their transition to traveling waves. This observation is in contrast to the transition behavior modeled

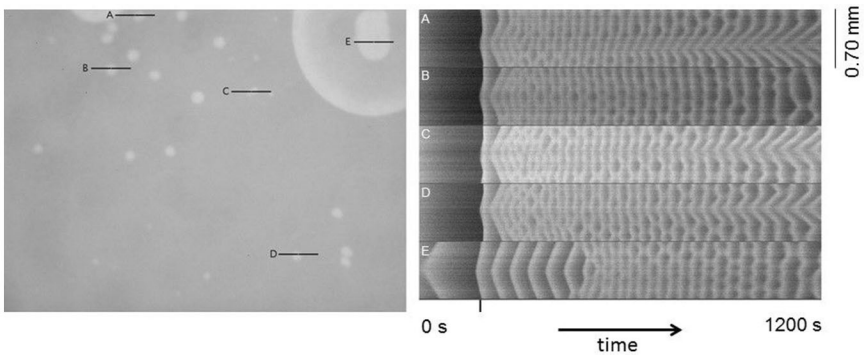

Figure 2. Invasion of modulated standing waves into the bulk oscillation region. The left image shows local spatial structures formed prior to the formation of the modulated standing waves. Image size is 7.11 mm 3 5.33 mm. This image was captured at the time marked in the space time plots on the right (184 s). The space-time plots on the right illustrate the evolution in time of the behavior on the individual lines A–E in the image on the left. Space time plots are each 0.70 mm 3 1200 s. The parameters w and f_d are 11.11 and 0.46, respectively.

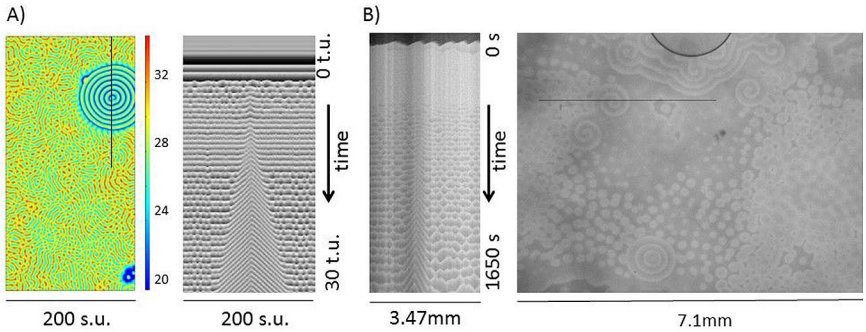

Figure 3. Death of standing waves. A) False color image on the left shows a numerical simulation of standing waves being overtaken by spirals in the Peña-Bestehorn model. The values of the variable U are indicated with the color bar. Numerical parameters are $A = 3$, $B = 5.6$, $p = 1$, $D_U = 5$, $D_V = 0.05$, $D_W = 1$. The initial conditions are set to the steady state for variables V and W, while U is perturbed from the steady state (Uss) to be U (x,y) = Uss + (1 + 0.1∗rnd(x, y)) where rnd(x, y) is the uniform random distribution with mean = 0 and range = 1. Space-time plot shows the evolution in time of the line of the image on the left. Image size is 200 3 400 space units. B) Experimental observations of standing waves overtaken by spirals are shown on the right. Experimental conditions are: [MA] = 0.25 M, [H_2SO_4] = 0.38 M, [$NaBrO_3$] = 0.2 M, [Ferroin] = 0.01 M . The parameters w and f_d are 10.07 and 0.44, respectively. Image size is 5.3 3 7.1 mm. Space-time plot on the left shows the evolution in time of the line in the image on the right.

and observed by Kaminaga *et al.*,[10] where the whole domain transitioned to traveling waves simultaneously.

4. Conclusions

In this paper, we have shown the invasion of the bulk medium by modulated standing waves, which are in turn overtaken by spirals. Invasion of standing waves has been reported previously in the BZ-AOT system[19] and in CO oxidation.[9] The invasion route here differs in the manner by which the standing waves invade, in this case behind a traveling wave front. We also report the observation of many nearly-simultaneously appearing localized structures prior to the spike of the relaxation oscillation. This phenomenon is consistent with the interpretation that at this point in the phase of oscillation, the oscillator is vulnerable to perturbation. Further work must be done to connect these results with Floquet analysis of a more chemically realistic model of this system.

In addition to invasion, we have qualitatively modeled the transition of standing waves to spiral traveling waves. This scenario differs from previous numerical and experimental work in that individual spiral structures form instead of the whole domain switching to traveling waves. The existing literature on standing wave defects is sparse, and we leave to future work the details of how individual defects form to allow spiral formation.

Turing patterns have been found experimentally in the present system[21,22] at lower H_2SO_4 concentrations. The invasion of Turing patterns into bulk oscillations has gathered recent interest.[23] Our interpretation of this invasion of standing waves into the bulk oscillation relies on the wave and Hopf instabilities, although additional interaction of the Turing instability could be responsible for the development of the lattice structure that develops after the first standing waves. Turing-wave interactions result in modulated standing waves as well.[24] Theory predicts that advection could be used to discriminate which instabilities are present under our conditions, which could be explored in future work.[25]

Acknowledgements

We acknowledge funding from the following NSF sources: Grants No. DMR-0820492, No. CHE-1362477, Graduate Research Fellowship No. 1102935. JS was supported by a Jordan-Dreyer Research Fellowship. We thank Tamás Bánsági Jr. and Viktor Horváth for advice and Francisco Mello, our machinist.

References

[1] A. M. Turing, *Philos. Trans. R. Soc. London Ser. B* **1952**, *237*, 37–72.
[2] V. Castets, E. Dulos, J. Boissonade, P. De Kepper P, *Phys. Rev. Lett.* **1990**, *64*, 2953–2956.
[3] B. Rudovics, E. Dulos, P. De Kepper, *Phys. Scr.* **1996**, *T67*, 43–50.
[4] D. G. Míguez, S. Alonso, A. P. Muñuzuri, F. Sagués, *Phys. Rev. Lett.* **2006**, *97*, 178301.
[5] S. Alonso, D. G. Míguez, F. Saguès, *Europhys. Lett.* **2008**, *81*, 30006.
[6] R. McIlwaine, V. K. Vanag, I. R. Epstein, *Phys. Chem. Chem. Phys.* **2009**, *11*, 1581.
[7] G. Heidemann, M. Bode, H.-G. Purwins, *Phys. Lett. A* **1993**, *177*, 225–230.
[8] S. Jakubith, H. H. Rotermund, W. Engel, A. von Oertzen, G. Ertl, *Phys. Rev. Lett.* **1990**, *65*, 3013–3016.

[9] A. von Oertzen, H. H. Rotermund, A. S. Mikhailov, G. Ertl, *J. Phys. Chem. B* **2000**, *104*, 3155–3178.
[10] A. Kaminaga, V. K. Vanag, I. R. Epstein, *Phys. Rev. Lett.* **2005**, *95*, 058302.
[11] T. Bánsági, V. K. Vanag, I. R. Epstein, *Phys. Rev. E* **2012**, *86*, 045202.
[12] V. K. Vanag, I. R. Epstein, *J. Chem. Phys.* **2004**, *121*, 890–894.
[13] B. Peña, M. Bestehorn, *Eur. Phys. J. Special Topics* **2007**, *146*, 301–311.
[14] B. Peña, C. Pèrez-García, M. Bestehorn, *Int. J. Bifurcation Chaos Appl. Sci. Eng.* **2004**, *14*, 3899–3907.
[15] L. Yang, I. Berenstein, I. R. Epstein, *Phys. Rev. Lett.* **2005**, *95*.
[16] N. Manz, O. Steinbock, *Chaos* **2006**, *16*, 037112.
[17] P. R. Bauer, A. Bonnefont, K. Krischer, *Sci. Rep.* **2015**, *5*, 16312.
[18] J. Wang, I. Mann, *J. Chem. Phys.* **2003**, *119*, 7924–7930.
[19] V. K. Vanag, I. R. Epstein, *Phys. Rev. Lett.* **2004**, *92*, 128301.
[20] I. Berenstein, *Chaos* **2015**, *25*, 064301.
[21] T. Bánsági, V. K. Vanag, I. R. Epstein, *Science* **2011**, *331*, 1309–12.
[22] V. K. Vanag, I. R. Epstein, *Phys. Rev. Lett.* **2001**, *87*, 228301.
[23] I. Berenstein, J. Carballido-Landeira, *RSC Adv.* **2016**, *6*, 56867–56873.
[24] L. Yang, M. Dolnik, A. M. Zhabotinsky, I. R. Epstein, *J. Chem. Phys.* **2002**, *117*, 7259.
[25] I. Berenstein, *Chaos* **2012**, *22*, 043109.

Received: December 19, 2017
Accepted: February 23, 2018
Published online on ■■, ■■■

FULL PAPER

*D. K. Gaskins, J. S. Soohoo, M. Dolnik, I. R. Epstein**

1 – 6

Birth and Death of Invading Standing Waves in the BZ-AOT Reaction-diffusion System